Research, Society and Development, v. 11, n. 2, e16511225556, 2022
(CC BY 4.0) | ISSN 2525-3409 | DOI: http://dx.doi.org/10.33448/rsd-v11i2.25556

Adsorption of acid yellow dye 17 on activated carbon prepared from *Euterpe oleracea*: kinetic and thermodynamic studies

Adsorção do corante amarelo ácido 17 em carvão ativado preparado do cacho do açaí *Euterpe oleracea*: estudos cinéticos e termodinâmico

Adsorción de colorante amarillo ácido 17 sobre carbón activado preparado a partir de *Euterpe oleracea*: estudios cinéticos y termodinámicos

Received: 01/10/2022 | Reviewed: 01/13/2022 | Accept: 01/20/2022 | Published: 01/22/2022

Deusimar de Oliveira Lopes
ORCID: https://orcid.org/0000-0003-2001-6301
Universidade Federal do Sul e Sudeste do Pará, Brazil
E-mail: deusimarc6h12o6@gmail.com
Lucas Oliveira Santos
ORCID: https://orcid.org/0000-0002-8525-520X
Universidade Federal do Sul e Sudeste do Pará, Brazil
E-mail: lucasuepa2016@outlook.com
Evair Dias Nascimento
ORCID: https://orcid.org/0000-0002-2821-2094
Universidade Federal de São Carlos, Brazil
E-mail: evair190@gmail.com
Adriane Damasceno Vieira de Souza
ORCID: https://orcid.org/0000-0003-1356-9573
Universidade Federal do Sul e Sudeste do Pará, Brazil
E-mail: adrianedamasceno@unifesspa.edu.br
Francisco Adriano de Oliveira Carvalho
ORCID: https://orcid.org/0000-0002-6025-4120
Universidade Federal do Sul e Sudeste do Pará, Brazil
E-mail: adriano.carvalho@unifesspa.edu.br

Abstract
Environmental pollution has been a point of discussion in the international community and an object of investigation by research groups, which focus on the development of remediation methods. In the current study, the bunch of açaí (*Euterpe oleracea*) was used as a precursor for the preparation of low-cost activated carbon in order to remove the dye 17 AY 17 from the aqueous solution. The synthesis was carried out at temperatures of 500, 600 and 700 °C, for 2.0 h in a muffle furnace. The kinetic and thermodynamic mechanism of the adsorption process of the acid yellow dye 17, and the effects of pH, contact time and initial concentration were investigated. Activated carbon carbonized at 700 °C had the highest adsorption capacity, about of 99.9% of removal of the AY. The adsorption capacity of AY 17 was slightly pH dependent with a maximum value at pH 2.0. The kinetic data show that the equilibrium time was 200 min, and the adsorption capacity of activated carbon was 99.9% at 50 mg L^{-1} and 67.0% at 150 mg L^{-1} of adsorbate, suggesting high adsorption capacity of the material, even in the presence of high dye concentration. The adsorption process of AY 17 is described by the pseudo-second order kinetic model, and the experimental adsorption isotherms are adjusted to the Freundlich model, indicating that the adsorption of AY 17 on activated carbon occurs with the formation of multilayers. The present study shows that this low-cost material has great potential for remediation of textile effluents.
Keywords: Adsorption; Activated carbon; Acid yellow 17.

Resumo
A poluição do meio ambiente tem sido ponto de discussão na comunidade internacional e objeto de investigação por grupos de pesquisa, que têm buscado o desenvolvimento de métodos de remediação. No presente estudo, o cacho de açaí (*Euterpe oleracea*) foi utilizado como precursor de carvão ativado de baixo custo para a remoção do corante amarelo ácido 17 (AY 17) em solução aquosa. A síntese foi realizada nas temperaturas de 500, 600 e 700 ° C, por 2,0 h em forno mufla. O mecanismo cinético e termodinâmico do processo de adsorção do corante AY 17, e os efeitos do pH, tempo de contato e concentração inicial foram investigados para o carvão ativado com maior capacidade adsortiva. O carvão ativado carbonizado a 700 °C teve a maior capacidade adsortiva, cerca de 99,9% de remoção do AY. A capacidade de adsorção de AY 17 é ligeiramente dependente do pH, com um valor máximo em pH 2,0. Os dados cinéticos mostram que o tempo de equilíbrio é de 200 min, e a capacidade de adsorção do carvão ativado foi de 99,9%

a 50 mg L^{-1} e 67,0% a 150 mg L^{-1} de adsorbato, sugerindo alta capacidade de adsorção do material, mesmo na presença de alta concentração de corante. O processo de adsorção de AY 17 é descrito pelo modelo cinético de pseudo-segunda ordem, e as isotermas experimentais de adsorção são ajustadas ao modelo de Freundlich, indicando que a adsorção de AY 17 no carvão ativado ocorre com a formação de multicamadas. O presente estudo mostra que esse material de baixo custo possui grande potencial para remediação de efluentes têxteis.
Palavras-chave: Adsorção; Carvão ativado; Amarelo ácido 17.

Resumen
La contaminación ambiental ha sido un punto de discusión en la comunidad internacional y objeto de estudio de diversos grupos de investigación, que se enfocan en el desarrollo de métodos de remediación. En el presente estudio, se utilizó el racimo de açaí (*Euterpe oleracea*) como precursor para la preparación de carbón activado de bajo costo, con el fin de eliminar el tinte amarillo ácido 17 (AY 17) en solución acuosa. La síntesis se llevó a cabo a temperaturas de 500, 600 y 700°C, durante 2,0 h en una mufla. El mecanismo cinético y termodinámico del proceso de adsorción del tinte AY 17, y los efectos del pH, el tiempo de contacto y la concentración inicial se investigaron utilizando el tipo de carbón activado con la mayor capacidad de remoción. El carbón activado a 700 °C tuvo la mayor capacidad de adsorción, con un 99,9% de remoción AY 17. La capacidad de adsorción del AY 17 fue ligeramente dependiente del pH, alcanzando un valor máximo a pH 2,0. Los datos cinéticos muestran que el tiempo de equilibrio fue de 200 min, y la capacidad de adsorción del carbón activado fue del 99,9% a 50 mg L^{-1} y del 67,0 % a 150 mg L^{-1} de adsorbato, sugiriendo una alta capacidad de adsorción del material, incluso en la presencia de una alta concentración de tinte. El proceso de adsorción de AY 17 se describe mediante el modelo cinético de pseudo-segundo orden, y las isotermas de adsorción experimentales se ajustan al modelo de Freundlich, lo que indica que la adsorción de AY 17 en carbón activado ocurre con la formación de multicapas. El presente estudio muestra que este material de bajo costo posee gran potencial para la remediación de efluentes textiles.
Palabras clave: Adsorción; Carbón activado; Amarillo ácido 17.

1. Introduction

The contamination and degradation of the environment by polluting gases, residues from agricultural activities, organic waste, toxic chemical products and other polluting sources has been the subject of debate in today's society (Chen *et al*., 2020; Khattab *et al*., 2020; Kishor *et al*., 2021; Nambela *et al*., 2020; Sarkar *et al*., 2017; Ignachewski *et al*., 2010). These pollutants promote an imbalance in the environment, and have reduced drastically the quality of available drinking water (Kishor *et al*., 2021; Munagapati *et al*., 2021; Hynes *et al*., 2020; Berradi *et al*., 2019; Sarkar *et al*., 2017; Ignachewski *et al*., 2010). Within the industrial sector, textiles are responsible for a large part of the economy of developed and some emerging countries *(Haseeb et al*., 2020). However, it is estimated that for the processing of about 12-20 tons of raw material are discarded daily between 1000 and 3000 m^3 of wastewater, thus promoting significant impacts on the environment (Ghaly, 2014). In addition, wastewater from activities in this sector has around 20% of dyes (Hynes *et al*., 2020; Khattab *et al*., 2020; Berradi *et al*., 2019), which are potentially toxic (Hynes *et al*., 2020; Benkhaya *et al*., 2020; Berradi *et al*., 2019; Verma *et al*., 2019; Obaid *et al*., 2016) generating negative impacts on the environment in terms of salinity, biological oxygen demand (BOD), chemical oxygen demand (COD), pH, temperature and others (Hynes *et al*., 2020; Berradi *et al*., 2019; Parveen & Rafique, 2018; Roy *et al*., 2018; Sarkar *et al*., 2017).

Several studies have shown that the treatment of these residues in effluents represents one of the great challenges of the textile sector, since these chemical substances have high chemical and biological stability, making their degradation difficult (Hynes *et al*., 2020; Khattab *et al*., 2020; Berradi *et al*., 2019; Obaid *et al*., 2016). In addition, the presence of color significantly contributes to the pollution of water resources by drastically reducing the penetration of sunlight, and consequently the photosynthesis capacity of aquatic plants and algae (Hynes *et al*., 2020; Benkhaya *et al*., 2020). On the other hand, the chemical activity of these substances in the human body can cause breathing difficulties, eye irritation, impairment of the cardiovascular system, mutations, tumors and affect the nervous system (Shindhal *et al*., 2021; Yusop *et al*., 2021; Bulca *et al*., 2021; Achour *et al*., 2021; Khatri *et al*., 2018; Hassaan *et al*., 2016; Vacchi *et al*., 2013). Therefore, many research groups have focused on the

development of efficient and low-cost methods that enable the removal and remediation of these pollutants, in order to alleviate possible environmental impacts and maintain the integrity of human health.

On the other hand, dyes are chemical substances that play an essential role in various industry sectors, such as textiles, printing, food, plastics, cosmetics and pharmaceutical industries, whose main objective is to add color to various products (Benkhaya et al., 2020; Berradi *et al*., 2019; Verma *et al*., 2019; Castro *et al*., 2018). These compounds are classified according to several criteria, including the chemical structure, which is made up of chromophore and auxochrome groups (Benkhaya et al., 2020; Berradi *et al*., 2019; Verma *et al*., 2019; Castro *et al*., 2018; Raman & Kanmani, 2016). Azo dyes, for example, which have the azo chromophore group (-N=N-) is the predominant class in the textile industry, representing 70% of the dyes used in this sector (Benkhaya *et al*., 2020; Berradi *et al*., 2019; Castro *et al*., 2018; Sarkar *et al*., 2017; Lang *et al*., 2013). This class of textile dye is highly water soluble and easily reacts with cellulosic, protein, polyester, acrylic and polyamide fibers *(*Castro *et al*., 2018; Guaratini & Zanoni, 2000).

Currently, several techniques are used in order to treat wastewater contaminated by dyes, including adsorption, coagulation, electrochemical treatment, photocatalytic degradation, ozone treatment and biological treatment (Achour *et al*., 2021; Shindhal *et al*., 2021; Yusop *et al*., 2021; Paredes-Quevedo *et al*., 2021; Verma *et al*., 2019; Khatri *et al*., 2018; Obaid *et al*., 2016;). However, a large portion are ineffective, as these substances have a very stable chemical structure and low biodegradation rate (Shindhal *et al*., 2021; Paredes-Quevedo *et al*., 2021; Benkhaya *et al*., 2020; Verma *et al*., 2019; Castro *et al*., 2018;). Among the most efficient techniques, adsorption stands out due to its ease of operation, simplicity of the project and, above all, to be economically viable (Achour *et al*., 2021; Bulca *et al*., 2021; Yusop *et al*., 2021; Paredes-Quevedo *et al*., 2021; Verma *et al*., 2019; Machrouhi *et al*., 2018), being, therefore, widely used to remove certain classes of contaminants from industrial effluents (Achour *et al*., 2021; Bulca *et al*., 2021; Yusop *et al*., 2021; Heidarinejad *et al*., 2020; Ugwu & Agunwamba, 2020; Alam *et al*., 2020; Machrouhi *et al*., 2018). Studies in the literature have reported several efficient materials in the removal of aqueous contaminants such as activated carbon, zeolites, clays, biomass, fungi and bacteria (Achour *et al*., 2021; Heidarinejad *et al*., 2020; Ani *et al*., 2020; Alkathiri *et al*., 2020; Machrouhi *et al*., 2018).

However, due to the high costs of commercial activated carbon, alternative adsorbents that guarantee the same adsorption efficiency have been studied, with emphasis on those produced from residues from agricultural and extractive activities (Achour *et al*., 2021; Alam *et al*., 2020; Alkathiri *et al*., 2020; Panwar and Pawar, 2020; Kannaujiya *et al*., 2021; Zoroufchi Benis *et al*., 2020; Reza *et al*., 2020). Several studies report the use of these materials in the synthesis of activated carbon for remediation of effluents, such as the study by Njoku *et al*. (2014) who studied the efficiency of activated carbon obtained from rambutan husk (*Nephelium lappaceum*) in the adsorption of acid yellow dye 17 (Reza *et al*., 2020). Other works address the removal of acid yellow dye 17 using activated carbon obtained from eggplant residues, achieving maximum removal of 99.58 % (Kannaujiya *et al*., 2021), and the removal of anionic acid yellow dye 17 using avocado seed powder, showing excellent removal over a wide pH (Munagapati *et al*., 2021), range and adsorption study of acid yellow dye 17 using activated carbon obtained from the rice husks, providing a maximum removal of 99.98% (Patil *et al*., 2015). However, most of these works use synthesis routes with inert gases, such as nitrogen and argon, which increase the cost of the process (Reza *et al*., 2020;.Patil *et al*., 2015).

In view of the aforementioned, this study focuses on synthesizing activated carbon in an open atmosphere, with high adsorption capacity, from açaí bunch (*Euterpe oleracea*), to remove the disodium dye 2.5-dichloro-4-[3-methyl -5-oxo-4-(4-sulfonatophenyl) diazenyl-diazyl-pyrazol-1-yl] benzenesulfonate in aqueous solution, commercially known as acid yellow 17, as well as characterize the kinetic and thermodynamic mechanism of adsorption.

2. Experimental Part

2.1 Preparation of dye stock solution Acid yellow 17

The acid yellow dye 17, namely (AY17) ($C_{16}H_{10}Cl_2N_4Na_2O_7S_2$), CAS number: 6359-98-4, ID 329751987, was purchased from Sigma-Aldrich company, Saint Louis, USA, at 60% content. This dye has an intense yellow color, being characterized by an absorption maximum around 402 nm, molar absorption coefficient 14,000.00 mol $^{-1}$ L cm^{-1} and molecular weight equal to 551.29 g mol $^{-1}$. Ultra-pure water with a resistivity of 18 MΩ cm, purified in a purifier (Milli-Q®, Merck Millipore), was used to prepare the solutions. The 1000 mg L^{-1} standard stock solution was prepared by dissolving 1.6 g of the dye in 1000 mL of ultrapure water. Then, the solution was properly stored for the studies.

2.2 Synthesis of adsorbents prepared from açaí bunch

The raw material (açaí bunches) collected in the municipality of Marabá-PA, was initially washed in running water to remove unwanted solid residues and subjected to a drying process at a temperature of 80 ºC in an (SSD-11L, Solidsteel) oven for 48 h. Then, the material was crushed in a knife mill model NL-226/02 (NewLab, Brazil) and classified in a Tyler-type sieve (Bertel, Brazil) coupled to a stirrer in the pass-through mesh range above 28 (0.25 mm). After classification, 50 g samples of biomass were carbonized in a Magnus brand muffle oven at temperatures of 500, 600, 700 ºC for 2.0 h and heating rate of 10 ºC min^{-1}. After the carbonization process, all samples were again classified in 325 mesh (0.044 mm) opening sieves and reserved for adsorption tests. The carbonized adsorbents at temperatures of 500, 600 and 700 ºC were named CA-CA500, CA-CA600 and CA-CA700 respectively.

2.3 Characterization of adsorbents by BE and BJH and IR

The textural properties of activated carbon were determined by adsorption-desorption of N_2 at 77.35 K using a surface analyzer (QUANTACHROME model NOVA 2200e) with liquid nitrogen of density 0.808 g cm^{-3}. Before taking the measurements, the sample was subjected to a thermal pre-treatment at 423 K for 2.0 h. The adsorption of N_2 in the sample was used to calculate the specific surface area (S_{BET}) by the BET method (Brunauer – Emmett – Teller), while the diameter (D_p) and pore volume (V_p) were determined by the BJH method (Barrett – Joyner – Halenda).

The infrared spectra of the *in natura* and carbonized samples and CA-CA700, both in a particle size of 325 meshes, were obtained by attenuated total reflectance (ATR), using a Thermo brand spectrometer, model Nicolet iS50 FT-IR, in the spectral region 4000-400 cm^{-1}, at 100 scans and 4 cm^{-1} resolution. Data acquisition was performed using the OMNIC program, and the treatment using the origin program, version 8.0. As a pre-treatment, the samples were dried at 105 °C for 24 hours.

2.4 Analytical curve

From the 1000 mg L^{-1} stock solution, solutions were prepared with a volume of 2.0 mL of the dye in the concentration range of 0 to 22 mg L^{-1} for the construction of the analytical curve. The UV-Vis experiments were carried out in a Bel Spectro S05 spectrophotometer, at the maximum absorption wavelength (λ_{max}) 400 nm. Sample absorbances were measured in a 1.0 mL quartz cuvette and 1.0 cm optical path.

2.5 Adsorption experiments

The adsorption measures were carried out in a 250 mL erlenmeyer flask, varying the mass of the adsorbents in the range of 0.1 to 1.0 g, in 100 mL of dye solution AY 17 in the concentration range of 25 to 300 mg L^{-1}, under stirring at 200 rpm at 20 °C.

Initially, measurements were taken to evaluate the most efficient adsorbent, in which 0.20 g of each synthesized material was exposed to 100 mL of the dye at 25 mg L^{-1}, under agitation in an orbital shaking incubator (SL-223) for 200 min, at pH 7.0. Adsorbent removal capacity (%) was measured using Equation 1:

$$\boldsymbol{Remo}\text{ção}\boldsymbol{o}(\%) = \frac{C_0 - C_e}{C_0} \times 100 \quad (1)$$

Where C_0 (mg L^{-1}) and C_e (mg L^{-1}) are the dye concentrations initially and at equilibrium, respectively (Munagapati *et al*., 2021).

In a second step, measurements were carried out to evaluate the effect of the adsorbent mass in the range (0.1 to 1.0 g), pH (2.0 to 9.0) and initial concentration of adsorbate (25 to 150 mg L^{-1}), under the same conditions as in step 1, at 20 °C and 200 rpm. The pH of the solutions was adjusted according to the studies by Salleh et al., 2011, Reza *et al*., 2020 and Salleh et al., 2011 in which small volumes of 0.1 mol L^{-1} HCl or 0.1 mol L^{-1} NaOH solutions were added until reaching the investigated pH value.

Therefore, the adsorption kinetics experiments of AY17 were carried out at concentrations of 50, 75, 100 and 150 mg L^{-1} and volume of 100 mL, in time intervals from 0 to 300 min, in the presence of 0.5 g of CA-CA700, at 20 °C, pH 6.0 and 200 rpm, while the equilibrium measurements were made with an interaction time of 200 min, in a wider concentration range, from 25 to 300 mg L^{-1}, to improve the acquisition of equilibrium isotherms. The ability to remove AY17 at equilibrium q_e (mg g^{-1}) was calculated from Equation 2:

$$\boldsymbol{q_e(mg\ g^{-1})} = \frac{[C_0(mg\ L^{-1}) - C_e(mg\ L^{-1})]V(L)}{m(g)} \quad (2)$$

where C_0 (mg L^{-1}) and C_e (mg L^{-1}) are the concentrations of the initial and equilibrium AY17 respectively, V (L) is the volume of solution and *m* (g) is the mass of adsorbent (Munagapati *et al*., 2021).

3. Results and Discussion

3.1 Adsorption efficiency of materials

Table 1 shows the adsorption capacity of the three adsorbents synthesized from the açaí bunch as a function of carbonization temperature.

Table 1 - Adsorption capacity of adsorbents obtained from the açaí bunch. Tests performed with 0.20 g of absorbent, at 20 ºC, pH 6.0, in the presence of 100 mL of AY17 solution, 25 mg L^{-1}, and contact time of 200 min.

Adsorbents	Mesh	Removal (%)
CA-CA500	325	38.0
CA-CA600	325	61.7
CA-CA700	325	99.9

Source: Authors (2021).

Under these conditions, the data show that the increase in temperature significantly contributes to the adsorption efficiency, with removal rates of 38.0, 61.7 and 99.9 % being observed for CA-CA500, CA-CA600 and CA-CA700, respectively (Table 1). The increase of 200 ºC granted an increase of 61.9 % in the AY17 removal (Table 1). This removal index obtained for the CA-CA700 is very similar to other studies such as Kannaujiya *et al*., 2021 and Patil *et al*., 2015. Studies in the literature

show that the increase in carbonization temperature produces two main effects, the first is the significant increase in the surface area of the carbonized material, and consequently a greater adsorption efficiency, and second, a significant loss of synthesis yield (Ani *et al*., 2020; Machrouhi *et al*., 2018), corroborating the data reported in the present study.

Thus, the following experiments were carried out only with the adsorbent with the highest adsorption capacity, CA-CA700.

3.2 CA-CA700 characterization

Figure 1 shows the adsorption-desorption isotherm of N_2 at 77 K for activated carbon from the açaí bunch (CA-CA700). A The isotherm obtained presents a characteristic profile of the type IV isotherm, according to the classification of the International Union of Pure and Applied Chemistry (IUPAC), (Foo and Hameed, 2012; Sing, 1982) with an H_4-type hysteresis cycle in the P/P_0 range from 0.4 to 0.99 , suggesting that the surface of CA-CA700 is predominantly constituted by mesopores (Munagapati *et al*., 2021; Sing, 1982; Shoaib *et al*., 2020; Hamza et al., 2018). The textural properties obtained by the BET and BJH methods, indicate that the material has a surface area of 353 $m^2 g^{-1}$, average pore diameter of 3.628 nm and pore volume of 0.046 $cm^3 g^{-1}$ corroborating the presence of mesopores in the structure, since for this type of isotherm the diameter range for mesoporous material is between 2.0 and 50 nm. (Munagapati *et al*., 2021; Shoaib *et al*., 2020; Mahmoud *et al*., 2020; Berradi *et al*., 2019; Jedynak *et al*., 2019; Hamza *et al*., 2018).

Figure 1 - N_2 adsorption-desorption isotherm for CA-CA700.

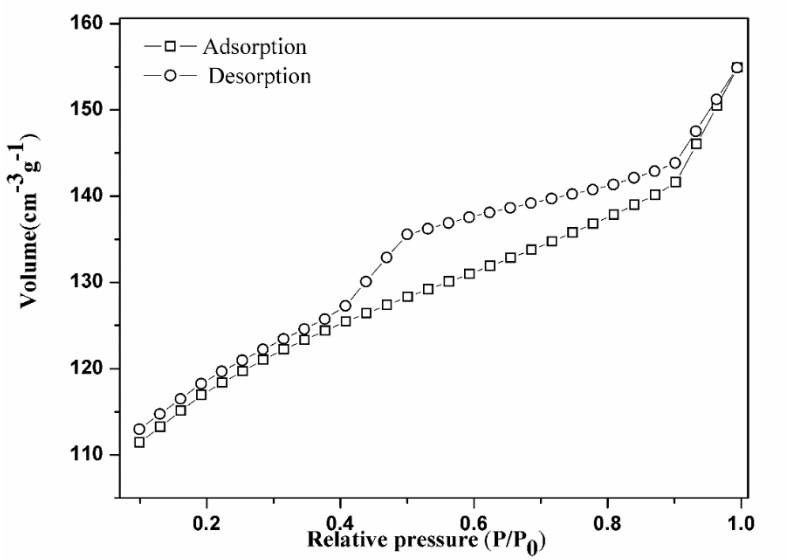

Source: Authors (2021).

The infrared spectra in the range from 4000 to 450 cm^{-1} for *in natura* sample of the açaí bunch and for the CA-CA700 adsorbent are shown in Figure 2. The FTIR spectrum of the açaí bunch biomass is characterized by the presence of a band of greater intensity at 3,385 cm^{-1} associated with the stretching of the hydroxyl group with hydrogen bonds in the cellulose (-OH). Other less intense bands centered at 2920 cm^{-1}, due to axial CH_2 deformation characteristic of the methyl group, 1740 cm^{-1} associated with the presence of the natural carbonyl group (C=O) of hemicellulose, 1610 cm^{-1} attributed to the stretching of the C bond = C of aromatic compounds, 1518 cm^{-1} contribution of primary and secondary amines, 1,160 and 1,056 cm^{-1} contribution of COC binding in hexoses, are observed. Carbonization promotes drastic changes in the functional groups of the biomass, characterized by an intense reduction in the contributions of oxygenated groups, which suggest the dehydration of the material.

The CA-CA700 spectrum presents bands at 1420, 1040 and 870 cm^{-1} that are associated with the cellulose structure and indicate the partial degradation of the material in pyrolysis.

Figure 2 - Infrared spectra for samples of açaí biomass *(Euterpe oleracea) in natura and carbonized* at 700 °C (CA-CA700).

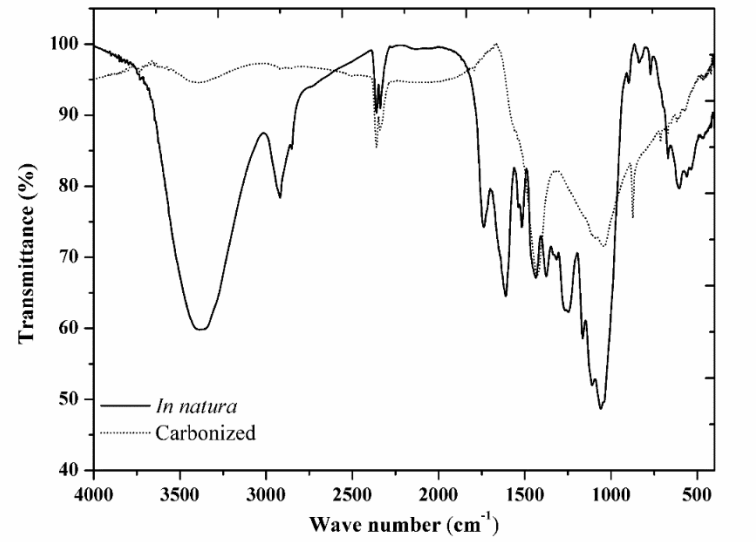

Source: Authors (2021).

3.3 Effect of contact time and initial concentrations on AY 17 adsorption

Figure 3 shows the effect of contact time (min) and initial concentrations in the adsorption process of acid yellow dye 17 for concentrations of 50, 75, 100 and 150 mg L^{-1}.

Figure 3 - Effect of initial concentrations and contact time on the adsorption process of AY 17, at 20 °C, 200 rpm, pH 6.0 and 0.5 g of CA-CA700.

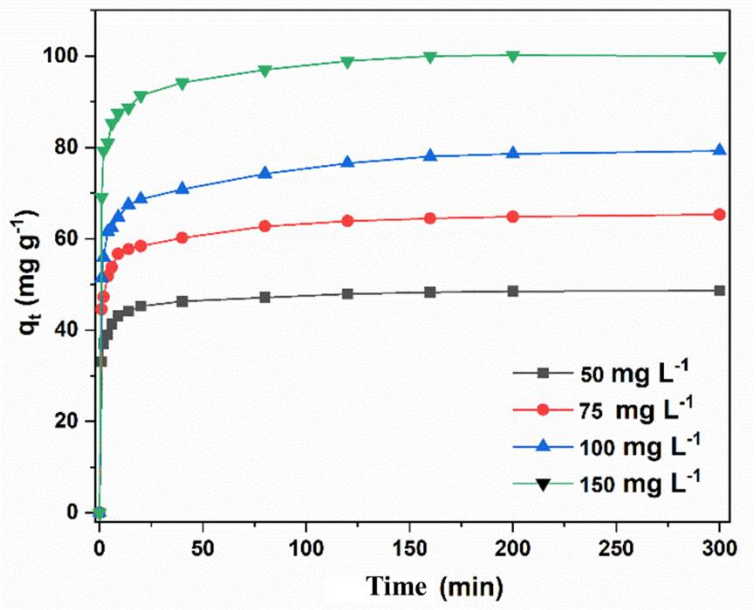

Source: Authors (2021).

At the beginning of the process, the adsorption rate increases rapidly up to 25 min, followed by a gradual increase until reaching the equilibrium state, in 200 min (Figure 3). (Munagapati *et al*., 2021; Reza *et al*., 2020; Abdulhameed *et al*., 2019).

The rapid adsorption of the dye at the beginning of the process is associated with the large availability of empty sites and the reduction in the rate with increasing interaction time indicates the increase in repulsive forces between the adsorbate molecules as the sites are occupied, as well as the saturation of the sites available for adsorption (Munagapati *et al*., 2021; Reza *et al*., 2020; Patil *et al*., 2015; Srivastava *et al.*, 2006). The adsorption capacity of CA-CA700 for acid yellow dye 17 increased from 47.9 ± 0.1 mg g^{-1} to 100.2 ± 0.2 mg g^{-1} when the initial concentration of dye increased from 50 to 150 mg L^{-1}, suggesting that this material is suitable for the treatment of textile effluents.

3.4 Effect of pH on adsorption

The effect of pH on the removal capacity of CA-CA700 is shown in Figure 4. The result shows that the AY 17 removal index decreases from 99 % at pH 2.0 to 92% at pH 9.0, indicating a promising applicability of the material under real conditions for textile effluents.

Figure 4. Effect of pH on the adsorption of AY 17, at 20 °C, 200 rpm, equilibrium time of 200 min, 0.5 g and 150 mg L^{-1}.

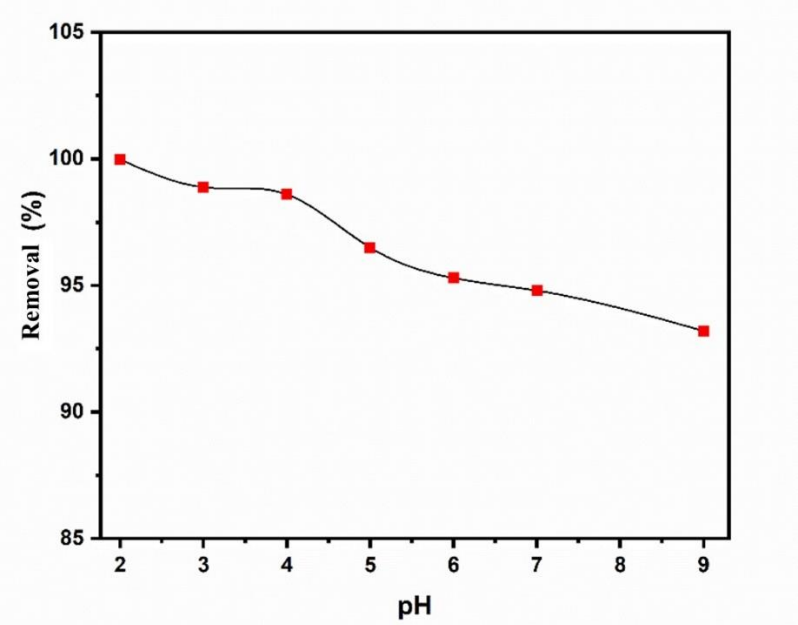

Source: Authors (2021).

According to the literature, adsorption is favored in an acidic medium for anionic dyes, because the surface protonation favors the interaction with the sulfonic groups of the dye through electrostatic forces (Bouhadjra *et al*., 2021; Felista *et al*., 2020; Jain *et al*., 2020; Cardoso *et al*., 2011). This phenomenon is due to the presence of sulfonate groups ($-SO_3Na$) in the structure of the acid yellow dye 17, which, in an aqueous medium, makes available the sulfonic groups ($-SO_3^-$), allowing the occurrence of electrostatic interactions with the functional groups present on the surface of the CA-CA700. At pH below 7.0, the initially negative functional groups of CA-CA700 are partially neutralized by the addition of protons (H^+), enabling an electrostatically favorable interaction of the adsorbent with the anionic form of the dye in an aqueous medium, thus increasing the index of removal (Bouhadjra *et al*., 2021; Bhomick *et al*., 2018; Li *et al*., 2018). Higher removal rates of the acid yellow dye 17 at lower pH values is in accordance with the study by Patil *et al*., 2015, using rice husk as an adsorbent, in which a removal of 72.1% was obtained at pH 2, value lower than that found in this study, being 99.8% at the same pH.

In addition, Reza et al., 2020 and Munagapati *et al*., 2021 studied the adsorption of AY 17 on activated carbon, with a high removal capacity being reported in the pH range between 2.0 and 7.0.

3.5 Kinetic models

The characterization of the adsorption kinetics provides important information about the adsorption mechanism, which is essential to evaluate the adsorption efficiency (Munagapati *et al*., 2021). Experimental data were fitted using pseudo-first-order and pseudo-second-order models. The linearized mathematical expression for the pseudo-first order model is shown in Equation 3 (Veit *et al*., 2014).

$$\ln(q_e - q_t) = lnq_e - k_1 t \quad (3)$$

where, q_t (mg g^{-1}) and q_e (mg g^{-1}) are the amount of solute adsorbed over time t and the amount adsorbed when equilibrium is reached, respectively, k_1 (min^{-1}) is the pseudo-first order adsorption rate constant and e *t* (min) is the contact time. Likewise, the linearized mathematical expression for pseudo-second order adsorption is shown in Equation 4.

$$\frac{t}{q_t} = \frac{1}{q_e^2 k_2} + \frac{1}{q_e} t \quad (4)$$

where k_2 (g mg^{-1} min^{-1}) is the pseudo-second order adsorption rate constant.

Figure 5 shows the fits using Equations 3 and 4 of the experimental data for the pseudo-first order (Figure 5a) pseudo-second order (Figure 5b) models. The kinetic parameters obtained from the adjustments are shown in Table 2.

From Figure 5a and the parameters presented in Table 2, the pseudo first order kinetic model is not adequate to describe the adsorption process of dye AY 17 in CA-CA700. Considering the linear regression coefficients (R^2_{adj}) for all concentrations in this study, the pseudo-second order model better describes the adsorption process of AY 17 and suggests that the dye adsorption rate on the surface of CA-CA700 is strongly dependent on the number of species adsorbed on the surface of the adsorbent (availability of free sites), than the concentration of dye in the solution (Table 2). This behavior is evidenced in the low dependence on the velocity constant (k_2), Table 2, as a function of concentration, in which almost no significant change is observed as a function of the concentration in the range from 75 to 150 mg L^{-1}.

Figure 5 - Adjustments to kinetic process of acid yellow dye 17 adsorption in CA-CA700, 0.5g, 20 °C at pH 6.0.

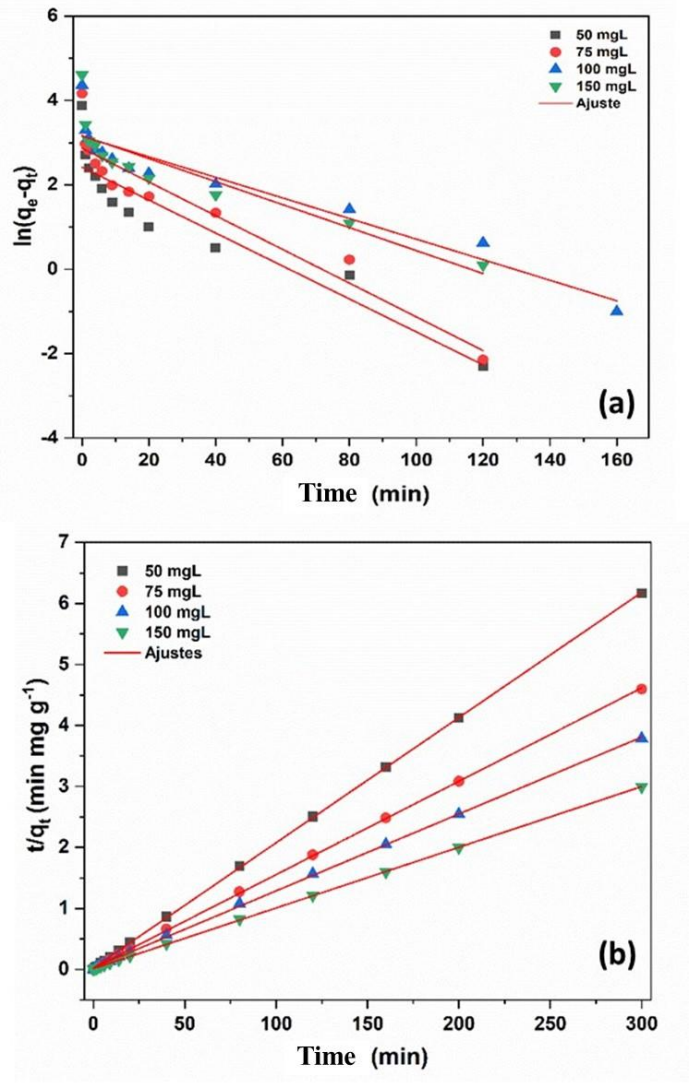

Source: Authors (2021).

Table 2 - Kinetic parameters for pseudo-first and pseudo-second orders models for acid yellow dye 17 (AY 17), 0.5 g of CA-CA700 at 20 °C, pH 6.0.

Co (mg L^{-1})	$q_{e,\,exp}$ (mg g^{-1})	*pseudo-first order*			*pseudo-second order*		
		k_1 (min^{-1}) x 10^{-3}	$q_{e1,\,cal}$ (mg g^{-1})	R^2_{adj}	k_2 (g mg^{-1}) x10^{-3}	$q_{e2,\,cal}$ (mg g^{-1})	R^2_{adj}
50.0	*47.9 ± 0.1*	*39 ± 5*	*11.2*	*0.8487*	*17 ± 2*	*48.7 ± 0.2*	*0.9999*
75.0	*64.1 ± 0.3*	*40 ± 4*	*17.6*	*0.8849*	*9.5 ± 0.5*	*65.3 ± 0.1*	*0.9998*
100.0	*78.7 ± 0.2*	*24 ± 3*	*23.3*	*0.8780*	*6 ± 1*	*79.3 ± 0.1*	*0.9996*
150.0	*100.2 ± 0.2*	*27 ± 4*	*23.7*	*0.7709*	*8 ± 1*	*100.4 ± 0.1*	*0.9999*

Source: Authors (2021).

Another parameter used to identify the kinetic controlling mechanism of the adsorption process is the proximity between the values of qe calculated by the theoretical ($q_{e,\,cal}$) and experimental ($q_{e,\,exp}$) model, in this case, the closer the proximity between these parameters, the greater it is the applicability of the model (Munagapati *et al*., 2021; Habibi *et al*., 2018). Table 2 shows that the values of $q_{e1,\,cal}$ obtained by the pseudo-first model are much lower than the values of $q_{e,\,exp}$ for all concentrations,

confirming that this model does not describe the kinetic mechanism of adsorption of AY 17 in CA -CA700. On the other hand, it was observed that the values of $q_{e2, cal}$ for the pseudo-second order model are very close to the experimental values, confirming that the adsorption process follows pseudo-second order kinetics. Studies in the literature for different dyes indicate that the adsorption process on activated carbon is described by the pseudo-second order model (Karthik *et al*., 2019). Njoku *et al*., 2014, studied the activated carbon adsorption kinetics of AY 17 in a concentration range of 50 to 400 mg L^{-1} and reported that the pseudo-second order model best describes the kinetic process of AY 17. Likewise, recent studies carried out by *Munagapati et al*., 2021 show that the adsorption of AY17 obeys the pseudo-second order model, with R^2_{adj} greater than 0.99 for six study temperatures. Other works involving adsorption of AY 17 on activated carbon also portray better adjustments to this model (Jedynak *et al*., 2019; Patil *et al*., 2015; Ahmad *et al*., 2014).

3.6 Adsorption isotherms

To evaluate the adsorption capacity of CA-CA700, adsorption isotherms obtained by the graphical relationship between q_e and C_e were used. The experimental data were adjusted according to the Langmuir, Freundlich and Temkin models, in order to obtain information regarding the specific surface properties and nature of the interactions between the adsorbate and the adsorbent (Munagapati *et al*., 2021; Njoku *et al*., 2014; Karthik *et al*., 2019). The Langmuir model (1918) suggests that the adsorption process occurs in monolayers and that the energy of the available sites is homogeneous (Njoku *et al*., 2014; Srivastava *et al*., 2006; Karthik *et al*., 2019). The mathematical expression for the linearized form of this model is shown in Equations 5 (Langmuir, 1918; Al-Ghouti & Da'ana, 2020).

$$\frac{C_e}{q_e} = \frac{1}{k_b q_m} + \frac{1}{q_m} C_e \quad (5)$$

where q_m (mg g^{-1}) and q_e (mg g^{-1}) are the maximum adsorption capacity per monolayer and the amount of solute adsorbed at equilibrium respectively, C_e (mg L^{-1}) is the concentration of adsorbate at equilibrium and k_b (L mg^{-1}) is the Langmuir constant associated with the free energy of the adsorption process.

Unlike the Langmuir model, the isotherm model proposed by Freundlich (1906) *(Munagapati et al., 2021; Karthik et al*., 2019); proposes that the adsorption occurs in multilayers, and that the adsorption energy decreases logarithmically as the surface of the adsorbent is covered (Munagapati *et al*., 2021; Kannaujiya *et al*., 2021; Njoku *et al*., 2014; Karthik *et al*., 2019; Al-Ghouti and Da'ana, 2020). Equation 6 shows the linearized form of the Freundlich model.

$$lnq_e = lnk_f + \frac{1}{n} lnC_e \quad (6)$$

Where k_f (mg g^{-1}) (L mg^{-1}) $^{1/n}$ and n are the Freundlich constant, related to adsorption capacity, and adsorption intensity, respectively (Al-Ghouti & Da'ana, 2020; Piccin *et al*., 2011; Inyinbor *et al*., 2016).

The Temkin isotherm model, on the other hand, assumes that the heat of adsorption of all molecules in the layer decreases linearly with surface coverage and that the adsorbent sites are heterogeneous (Njoku *et al*., 2014; Inyinbor *et al*., 2016; Mane *et al*., 2007; Kataria *et al*., 2016). The mathematical expression of this model is shown in equation 07 (Saadi *et al*., 2015).

$$q_e = Bln(AC_e) \quad (7)$$

In linearized form, the equation that describes the Temkin isotherm is commonly expressed as:

$$q_e = B\ lnA + B\ lnC_e \quad (8)$$

where B = RT/b and b (J mol $^{-1}$) is the Temkin constant related to the heat of adsorption, A (L g $^{-1}$) is the Temkin isotherm constant, R (8.314 J mol $^{-1}$ K $^{-1}$) is the universal gas constant and T (K) is the absolute temperature (Njoku *et al*., 2014; Piccin *et al*., 2011; Inyinbor *et al*., 2016; Kataria *et al*., 2016).

The adjustments using the Langmuir, Freundlich and Temkin (Saadi *et al*., 2015) models for the adsorption of AY 17 at 20 ºC, obtained from Equations 5, 6 and 8, are shown in Figure 6. The parameters obtained from the adjustments are shown in Table 3. The results show that the adsorption equilibrium data of AY17 is better described by the Freundlich model, whose R^2_{adj} of the adjustments was 0.9873 and the adsorption capacity constant k_f equal to 47.9 (mg g^{-1}) (L mg^{-1})$^{1/n}$ (Table 3). The value of the Freundlich constant (n) equal to 5.95 suggests that the adsorption process between AY 17 and CA-CA700 is favorable, because the higher the value of n (smaller the 1/n ratio), the stronger it is the interaction between the adsorbate and the adsorbent (Obaid *et al*., 2016; Lang *et al*., 2013; Al-Ghouti and Da'ana, 2020; Piccin *et al*., 2011; Inyinbor *et al*., 2016; Saadi *et al*., 2015; Delle Site, 2001). In addition, this model assumes that the process of adsorption of AY17 occurs mostly in multilayers (Njoku *et al*., 2014; Patil *et al*., 2015; Ahmad *et al*., 2014; Ashraf *et al*., 2013), a non-homogeneous surface, where the energy distribution in the sites is heterogeneous and strictly exponential (Al-Ghouti and Da'ana, 2020; Piccin *et al*., 2011; Inyinbor *et al*., 2016; Delle Site, 2001; Febrianto *et al*., 2009; Ahmad *et al*., 2014). Patil *et al*., 2015 when studying the models of Langmuir and Freundlich in the adsorption of dye AY 17, they also identified that the Freundlich model, in its linearized form, better adjusted to the experimental data, obtaining n equal to 1.85 and R^2_{adj} equal to 0.996 confirming that the adsorption of AY 17 occurs preferentially in multilayers. Ashraf *et al*., 2013 studied the adsorption of AY 17 on activated carbon produced from *T. Angustata L*. finding excellent fits to the Freundlich model.

Figure 6 - Linear adjustment by Langmuir, Freundlich and Temkin models of the adsorption isotherm of AY 17 at 20 °C, Ph 6.0 and 0.5 g of CA-CA700.

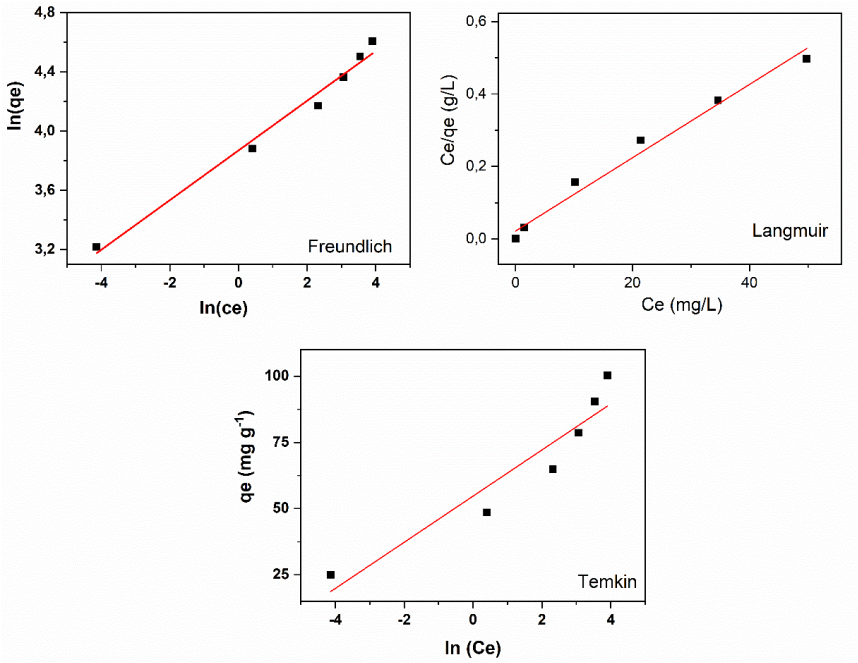

Source: Authors (2021).

Table 3 - Adjustment parameters for the acid yellow dye adsorption isotherm models 17 at 20 °C, *pH 6.0 and 0.5 g of* CA-CA700.

Langmuir			*Freundlich*			*Temkin*		
K_b *(L mg^{-1})*	q_m *(mg g^{-1})*	R^2_{adj}	k_f *	*n*	R^2_{adj}	*A (L g^{-1})*	*B (J mol^{-1})*	R^2_{adj}
0.467	*98.8*	*0.9236*	*47.9*	*5.95*	*0.9873*	*537.5*	*280*	*0.8717*

* (mg g^{-1}) (L mg^{-1})$^{1/n}$. Source: Authors (2021).

4. Conclusion

The data reported in this study indicated that the charcoal produced from the açaí bunch in an open atmosphere, without the use of inert gases that make the synthesis route more expensive, is promising for the treatment of effluents and, therefore, is an important alternative for the reduction of these waste in the environment. CA-CA700 is effective for the removal of acid yellow 17, showing high adsorptive capacity under the conditions studied. The equilibrium time is reached with 200 min and the adsorption process of AY 17 in the CA-CA700 is described by the pseudo-second order kinetic model while the Freundlich isotherm model indicates that the interaction between adsorbent and adsorbate is favorable and occurs in multilayers.

Our results represent a nice contribution and an important and necessary step in the low-cost materials adsorbents for removal dyes in the aqueous solutions. In future publications, the authors propose the use of adsorbent materials obtained from the plant biomass of the Amazon biome, mainly from extractivism, and composite materials for the treatment of textile effluents, heavy metals, drugs and other contaminants in water bodies and soil.

Acknowledgments

The authors are grateful to the Ceramic Materials Synthesis Laboratory (LABSMAC, Campina Grande, Brazil) for making available the BET and FTIR facilities used in this work. Thanks are due to the Brazilian agencies CNPq (Process number nº 407891/2018-8), and CAPES for partial financial support. Lucas O. Santos is the recipient of an M.Sc. grant from CAPES (Finance Code 001).

References

Abdulhameed, A. S., Mohammad, A. K. T., & Jawad, A. H. (2019). Application of response surface methodology for enhanced synthesis of chitosan tripolyphosphate/TiO2 nanocomposite and adsorption of reactive orange 16 dye. *J. Clean. Prod*., 232, 43–56. https://doi.org/10.1016/j.jclepro.2019.05.291.

Achour, Y., Bahsis, L., Ablouh, E. H., Yazid, H., Laamari, M. R., & Haddad, M. El (2021). Insight into adsorption mechanism of Congo red dye onto Bombax Buonopozense bark Activated-carbon using Central composite design and DFT studies. *Surfaces and Interfaces*, 23, 100977. https://doi.org/10.1016/j.surfin.2021.100977.

Ahmad, M. A., Ahmad Puad, N. A., & Bello, O. S. (2014). Kinetic, equilibrium and thermodynamic studies of synthetic dye removal using pomegranate peel activated carbon prepared by microwave-induced KOH activation. *Water Resour. Ind*., 6, 18–35. https://doi.org/10.1016/j.wri.2014.06.002.

Al-Ghouti, M. A., & Da'ana, D. A. (2020). Guidelines for the use and interpretation of adsorption isotherm models: A review. *J. Hazard. Mater*., 393, 122383. https://doi.org/10.1016/j.jhazmat.2020.122383.

Alam, M. M., Hossain, M. A., Hossain, M. D., Johir, M. A. H., Hossen, J., Rahman, M. S., Zhou, J. L., Hasan, A. T. M. K., Karmakar, A. K., & Ahmed, M. B. (2020). The potentiality of rice husk-derived activated carbon: From synthesis to application. *Processes*, 8. https://doi.org/10.3390/pr8020203.

Alkathiri, D. S. S., Sabri, M. A., Ibrahim, T. H., ElSayed, Y. A., & Jumean, F. (2020). Development of activated carbon fibers for removal of organic contaminants. *Int. J. Environ. Sci. Technol.*, 17, 4841–4852. https://doi.org/10.1007/s13762-020-02808-8.

Ani, J. U., Akpomie, K. G., Okoro, U. C., Aneke, L. E., Onukwuli, O. D., & Ujam, O. T. (2020). Potentials of activated carbon produced from biomass materials for sequestration of dyes, heavy metals, and crude oil components from aqueous environment. *Appl. Water Sci*., 10, 1–11. https://doi.org/10.1007/s13201-020-1149-8.

Ashraf, M. A., Hussain, M., Mahmood, K., Wajid, A., Yusof, M., Alias, Y., & Yusoff, I. (2013). Removal of acid yellow-17 dye from aqueous solution using eco-friendly biosorbent. Desalin. *Water Treat.*, 51, 4530–4545. https://doi.org/10.1080/19443994.2012.747187.

Benkhaya, S., M' rabet, S., & El Harfi, A. (2020). A review on classifications, recent synthesis and applications of textile dyes. *Inorg. Chem. Commun*., 115, 107891. https://doi.org/10.1016/j.inoche.2020.107891.

Berradi, M., Hsissou, R., Khudhair, M., Assouag, M., Cherkaoui, O., El Bachiri, A., & El Harfi, A. (2019). Textile finishing dyes and their impact on aquatic environs. *Heliyon*, 5. https://doi.org/10.1016/j.heliyon.2019.e02711.

Bhomick, P. C., Supong, A., Baruah, M., Pongener, C., & Sinha, D. (2018). Pine Cone biomass as an efficient precursor for the synthesis of activated biocarbon for adsorption of anionic dye from aqueous solution: Isotherm, kinetic, thermodynamic and regeneration studies. *Sustain. Chem. Pharm.*, 10, 41–49. https://doi.org/10.1016/j.scp.2018.09.001.

Bouhadjra, K., Lemlikchi, W., Ferhati, A., & Mignard, S. (2021). Enhancing removal efficiency of anionic dye (Cibacron blue) using waste potato peels powder. *Sci. Rep*., 11, 1–10. https://doi.org/10.1038/s41598-020-79069-5.

Bulca, Ö., Palas, B., Atalay, S., & Ersöz, G. (2021). Performance investigation of the hybrid methods of adsorption or catalytic wet air oxidation subsequent to electrocoagulation in treatment of real textile wastewater and kinetic modelling. *J. Water Process Eng*., 40. https://doi.org/10.1016/j.jwpe.2020.101821.

Castro, A. S., Franco, C. R., & Cidade, M. J. A. (2018). Adsorption of dyes indosol blue, Indosol orange and drimarene red in aqueous solution by white clay. *Rev. Virtual Quim*., 10, 1502–1515. https://doi.org/10.21577/1984-6835.20180102.

Chen, F., Zhu, J., Yang, Y., & Wang, L. (2020). Assessing environmental impact of textile production with water alkalization footprint. *Sci. Total Environ*., 719, 137522. https://doi.org/10.1016/j.scitotenv.2020.137522.

Delle Site, A. (2001). Factors affecting sorption of organic compounds in natural sorbent/water systems and sorption coefficients for selected pollutants. A review. *J. Phys. Chem. Ref. Data*, 30, 187–439. https://doi.org/10.1063/1.1347984.

Febrianto, J., Kosasih, A. N., Sunarso, J., Ju, Y. H., Indraswati, N., & Ismadji, S. (2009). Equilibrium and kinetic studies in adsorption of heavy metals using biosorbent: A summary of recent studies. *J. Hazard. Mater*., 162, 616–645. https://doi.org/10.1016/j.jhazmat.2008.06.042.

Felista, M. M., Wanyonyi, W. C., & Ongera, G. (2020). Adsorption of anionic dye (Reactive black 5) using macadamia seed Husks: Kinetics and equilibrium studies. *Sci. African*, 7, e00283. https://doi.org/10.1016/j.sciaf.2020.e00283.

Foo, K. Y., & Hameed, B. H. (2012). Preparation of activated carbon by microwave heating of langsat (Lansium domesticum) empty fruit bunch waste. *Bioresour. Technol*., 116, 522–525. https://doi.org/10.1016/j.biortech.2012.03.123.

Guaratini, C. C. I., & Zanoni, M. V. B. (2000). Corantes têxteis. *Quim. Nova*, 23, 71–78.

Habibi, A., Belaroui, L.S., Bengueddach, A., López Galindo, A., Sainz Díaz, C. I., & Peña, A. (2018). Adsorption of metronidazole and spiramycin by an Algerian palygorskite. Effect of modification with tin. *Microporous Mesoporous Mater*., 268, 293–302. https://doi.org/10.1016/j.micromeso.2018.04.020.

Hamza, W., Dammak, N., Hadjltaief, H. B., Eloussaief, M., & Benzina, M. (2018). Sono-assisted adsorption of Cristal Violet dye onto Tunisian Smectite Clay: Characterization, kinetics and adsorption isotherms. *Ecotoxicol. Environ. Saf*., 163, 365–371. https://doi.org/10.1016/j.ecoenv.2018.07.021.

Haseeb, M., Kot, S., Hussain, H. I., Mihardjo, L. W. W., & Saluga, P. (2020). Modelling the non-linear energy intensity effect based on a quantile-on-quantile approach: The case of textiles manufacturing in asian countries. *Energies*, 13. https://doi.org/10.3390/en13092229.

Hassaan, M. A., Nemr, A. El, & Madkour, F. F. (2016). Application of Ozonation and UV assisted Ozonation for Decolorization of Direct Yellow 50 in Sea water. *Pharm. Chem. J*., 3, 131–138.

Heidarinejad, Z., Dehghani, M. H., Heidari, M., Javedan, G., Ali, I., & Sillanpää, M. (2020). Methods for preparation and activation of activated carbon: a review. *Environ. Chem. Lett*., 18, 393–415. https://doi.org/10.1007/s10311-019-00955-0.

Hynes, N. R. J., Kumar, J. S., Kamyab, H., Sujana, J. A. J., Al-Khashman, O. A., Kuslu, Y., Ene, A., & Suresh Kumar, B. (2020). Modern enabling techniques and adsorbents based dye removal with sustainability concerns in textile industrial sector -A comprehensive review. *J. Clean. Prod*., 272, 122636. https://doi.org/10.1016/j.jclepro.2020.122636.

Ignachewski, F., Fujiwara, T., Química, D. De, Centro-oeste, U.E., Camargo, R., Sá, V. De, Pr, G., Física, D. De, Centro-oeste, U.E., Camargo, R., Sá, V. De, Pr, G., Carneiro, L.M., & Tauchert, E. (2010). Degradação de corantes reativos por processo foto-fenton envolvendo o uso de peneira molecular 4a modificada com fe^{3+}. *Quim. Nova*, 33, 1640–1645.

Inyinbor, A. A., Adekola, F. A., & Olatunji, G. A. (2016). Kinetics, isotherms and thermodynamic modeling of liquid phase adsorption of Rhodamine B dye onto Raphia hookerie fruit epicarp. *Water Resour. Ind*., 15, 14–27. https://doi.org/10.1016/j.wri.2016.06.001.

Langmuir, I. (1918). Adsorption of Gases on Glass, Mica and Platinum. the Adsorption of Gases on Plane Surfaces of Glass, Mica and Platinum. *J. Am. Chem. Soc*., 40, 1361–1403.

Jain, S. N., Tamboli, S. R., Sutar, D. S., Jadhav, S. R., Marathe, J. V., Shaikh, A. A., & Prajapati, A. A. (2020). Batch and continuous studies for adsorption of anionic dye onto waste tea residue: Kinetic, equilibrium, breakthrough and reusability studies. *J. Clean. Prod*., 252, 119778. https://doi.org/10.1016/j.jclepro.2019.119778.

Jedynak, K., Wideł, D., & Rędzia, N. (2019). Removal of rhodamine b (A basic dye) and acid yellow 17 (an acidic dye) from aqueous solutions by ordered mesoporous carbon and commercial activated carbon. *Colloids and Interfaces*, 3. https://doi.org/10.3390/colloids3010030.

Kannaujiya, M. C., Prajapati, A. K., Mandal, T., Das, A. K., & Mondal, M. K. (2021). Extensive analyses of mass transfer, kinetics, and toxicity for hazardous acid yellow 17 dye removal using activated carbon prepared from waste biomass of Solanum melongena. *Biomass Convers. Biorefinery*., https://doi.org/10.1007/s13399-020-01160-8.

Karthik, V., Saravanan, K., Patra, C., Ushadevi, B., Vairam, S., & Selvaraju, N. (2019). Biosorption of Acid Yellow 12 from simulated wastewater by non-viable T. harzianum: kinetics, isotherm and thermodynamic studies. *Int. J. Environ. Sci. Technol*., 16, 6895–6906. https://doi.org/10.1007/s13762-018-2073-4.

Kataria, N., Garg, V. K., Jain, M., & Kadirvelu, K. (2016). Preparation, characterization and potential use of flower shaped Zinc oxide nanoparticles (ZON) for the adsorption of Victoria Blue B dye from aqueous solution. *Adv. Powder Technol*., 27, 1180–1188. https://doi.org/10.1016/j.apt.2016.04.001.

Khatri, J., Nidheesh, P. V., Anantha Singh, T. S., & Suresh Kumar, M. (2018). Advanced oxidation processes based on zero-valent aluminium for treating textile wastewater. *Chem. Eng. J.*, 348, 67–73. https://doi.org/10.1016/j.cej.2018.04.074.

Khattab, T. A., Abdelrahman, M. S., & Rehan, M. (2020). Textile dyeing industry: environmental impacts and remediation. *Environ. Sci. Pollut. Res*., 27, 3803–3818. https://doi.org/10.1007/s11356-019-07137-z.

Kishor, R., Purchase, D., Saratale, G. D., Saratale, R. G., Ferreira, L. F. R., Bilal, M., Chandra, R., & Bharagava, R. N. (2021). Ecotoxicological and health concerns of persistent coloring pollutants of textile industry wastewater and treatment approaches for environmental safety. *J. Environ. Chem. Eng*., 9, 105012. https://doi.org/10.1016/j.jece.2020.105012.

Lang, W., Sirisansaneeyakul, S., Ngiwsara, L., Mendes, S., Martins, L.O., Okuyama, M., & Kimura, A. (2013). Characterization of a new oxygen-insensitive azoreductase from Brevibacillus laterosporus TISTR1911: Toward dye decolorization using a packed-bed metal affinity reactor. *Bioresour. Technol*., 150, 298–306. https://doi.org/10.1016/j.biortech.2013.09.124.

Li, J., Wang, S., Peng, J., Lin, G., Hu, T., & Zhang, L. (2018). Selective Adsorption of Anionic Dye from Solutions by Modified Activated Carbon. *Arab. J. Sci. Eng*., 43, 5809–5817. https://doi.org/10.1007/s13369-017-3006-0.

Machrouhi, A., Farnane, M., Elhalil, A., Elmoubarki, R., Abdennouri, M., Barka, N., Qourzal, S., & Tounsadi, H. (2018). Effectiveness of beetroot seeds and H3PO4 activated beetroot seeds for the removal of dyes from aqueous solutions. *J. Water Reuse Desalin*., 8, 522–531. https://doi.org/10.2166/wrd.2017.034.

Mahmoud, M. E., Abdelfattah, A. M., Tharwat, R. M., & Nabil, G. M. (2020). Adsorption of negatively charged food tartrazine and sunset yellow dyes onto positively charged triethylenetetramine biochar: Optimization, kinetics and thermodynamic study. *J. Mol. Liq*., 318, 114297. https://doi.org/10.1016/j.molliq.2020.114297.

Mane, V. S., Mall, I. D., & Srivastava, V. C. (2007). Use of bagasse fly ash as an adsorbent for the removal of brilliant green dye from aqueous solution. *Dye. Pigment*., 73, 269–278. https://doi.org/10.1016/j.dyepig.2005.12.006.

Munagapati, V. S., Wen, H. Y., Vijaya, Y., Wen, J. C., Wen, J. H., Tian, Z., Reddy, G. M., & Raul Garcia, J. (2021). Removal of anionic (Acid Yellow 17 and Amaranth) dyes using aminated avocado (Persea americana) seed powder: adsorption/desorption, kinetics, isotherms, thermodynamics, and recycling studies. *Int. J. Phytoremediation*, 23, 911–923. https://doi.org/10.1080/15226514.2020.1866491.

Nambela, L., Haule, L.V., & Mgani, Q. (2020). A review on source, chemistry, green synthesis and application of textile colorants. *J. Clean. Prod*., 246, 119036. https://doi.org/10.1016/j.jclepro.2019.119036.

Njoku, V. O., Foo, K. Y., Asif, M., & Hameed, B. H. (2014). Preparation of activated carbons from rambutan (Nephelium lappaceum) peel by microwave-induced KOH activation for acid yellow 17 dye adsorption. *Chem. Eng. J*., 250, 198–204. https://doi.org/10.1016/j.cej.2014.03.115.

Obaid, M. K., Abdullah, L. C., & Idan, I. J. (2016). Removal of Reactive Orange 16 Dye from Aqueous Solution by Using Modified Kenaf Core Fiber. *J. Chem*., 2016, 1–8. https://doi.org/10.1155/2016/4262578.

Panwar, N. L., & Pawar, A. (2020). Influence of activation conditions on the physicochemical properties of activated biochar: a review. *Biomass Convers. Biorefinery*., https://doi.org/10.1007/s13399-020-00870-3.

Paredes-Quevedo, L. C., González-Caicedo, C., Torres-Luna, J. A., & Carriazo, J. G. (2021). Removal of a Textile Azo-Dye (Basic Red 46) in Water by Efficient Adsorption on a Natural Clay. *Water. Air. Soil Pollut*., 232. https://doi.org/10.1007/s11270-020-04968-2.

Parveen, K., & Rafique, U. (2018). Development of cobalt-doped alumina hybrids for adsorption of textile effluents. *Adsorpt. Sci. Technol*., 36, 182–197. https://doi.org/10.1177/0263617416687563.

Patil, C., Ratnamala, G. M., Channamallayya, S. T., & Belagavi, K. (2015). Adsorption Studies for Removal of Acid yellow 17 using Activated Rice Husk. *Inter. Res. J. of Eng. and Techn.*, 769–774.

Piccin, J. S., Dotto, G. L., & Pinto, L. A. A. (2011). Adsorption isotherms and thermochemical data of FDandC RED N° 40 Binding by chitosan. *Brazilian J. Chem. Eng*., 28, 295–304. https://doi.org/10.1590/S0104-66322011000200014.

Ghaly A. E, Ananthashankar R, Alhattab M, & Ramakrishnan V. V (2014). Production, Characterization and Treatment of Textile Effluents: A Critical Review. *J. Chem. Eng. Process Technol*., 05. https://doi.org/10.4172/2157-7048.1000182.

Raman, C. D., & Kanmani, S. (2016). Textile dye degradation using nano zero valent iron: A review. *J. Environ. Manage*., 177, 341–355. https://doi.org/10.1016/j.jenvman.2016.04.034.

Reza, M. S., Yun, C. S., Afroze, S., Radenahmad, N., Bakar, M. S. A., Saidur, R., Taweekun, J., & Azad, A. K. (2020). Preparation of activated carbon from biomass and its' applications in water and gas purification, a review. *Arab J. Basic Appl. Sci*., 27, 208–238. https://doi.org/10.1080/25765299.2020.1766799.

Roy, U., Sengupta, S., Das, P., Bhowal, A., & Datta, S. (2018). Integral approach of sorption coupled with biodegradation for treatment of azo dye using Pseudomonas sp.: batch, toxicity, and artificial neural network. *3 Biotech*, 8, 1–11. https://doi.org/10.1007/s13205-018-1215-1.

Saadi, R., Saadi, Z., Fazaeli, R., & Fard, N. E. (2015). Monolayer and multilayer adsorption isotherm models for sorption from aqueous media. *Korean J. Chem. Eng*., 32, 787–799. https://doi.org/10.1007/s11814-015-0053-7.

Salleh, M. A. M., Mahmoud, D. K., Karim, W. A. W. A., & Idris, A. (2011). Cationic and anionic dye adsorption by agricultural solid wastes: A comprehensive review. *Desalination*, 280, 1–13. https://doi.org/10.1016/j.desal.2011.07.019.

Sarkar, S., Banerjee, A., Halder, U., Biswas, R., & Bandopadhyay, R. (2017). Degradation of Synthetic Azo Dyes of Textile Industry: a Sustainable Approach Using Microbial Enzymes. *Water Conserv. Sci. Eng*., 2, 121–131. https://doi.org/10.1007/s41101-017-0031-5.

Shindhal, T., Rakholiya, P., Varjani, S., Pandey, A., Ngo, H. H., Guo, W., Ng, H. Y., & Taherzadeh, M. J. (2021). A critical review on advances in the practices and perspectives for the treatment of dye industry wastewater. *Bioengineered*, 12, 70–87. https://doi.org/10.1080/21655979.2020.1863034.

Shoaib, A. G. M., El-Sikaily, A., El Nemr, A., & Mohamed, A. E. D. A., Hassan, A. A. (2020). Preparation and characterization of highly surface area activated carbons followed type IV from marine red alga (Pterocladia capillacea) by zinc chloride activation. *Biomass Convers. Biorefinery*., https://doi.org/10.1007/s13399-020-00760-8.

Sing, K. S. W. (1982). Reporting physisorption data for gas / solid systems with Special Reference to the Determination of S. *Pure Appl. Chem*., 54, 2201–2218.

Srivastava, V. C., Swamy, M. M., Mall, I. D., Prasad, B., & Mishra, I. M. (2006). Adsorptive removal of phenol by bagasse fly ash and activated carbon: Equilibrium, kinetics and thermodynamics. *Colloids Surfaces A Physicochem. Eng. Asp*., 272, 89–104. https://doi.org/10.1016/j.colsurfa.2005.07.016.

Ugwu, E. I., & Agunwamba, J. C. (2020). A review on the applicability of activated carbon derived from plant biomass in adsorption of chromium, copper, and zinc from industrial wastewater. *Environ. Monit. Assess*., 192. https://doi.org/10.1007/s10661-020-8162-0.

Vacchi, F. I., Albuquerque, A. F., Vendemiatti, J. A., Morales, D. A., Ormond, A. B., Freeman, H. S., Zocolo, G. J., Zanoni, M. V. B., & Umbuzeiro, G. (2013). Chlorine disinfection of dye wastewater: Implications for a commercial azo dye mixture. *Sci. Total Environ*., 442, 302–309. https://doi.org/10.1016/j.scitotenv.2012.10.019.

Veit, M. T., Bedin, S., Gonçalves, G. C., Palácio, S. M., & Fagundes-Klen, M. R. (2014). Utilização do resíduo de erva-mate como material adsorvente do corante azul de metileno. *Eclet. Quim*., 39, 227–243.

Verma, K., Saha, G., Kundu, L. M., & Dubey, V. K. (2019). Biochemical characterization of a stable azoreductase enzyme from Chromobacterium violaceum: Application in industrial effluent dye degradation. *Int. J. Biol. Macromol*., 121, 1011–1018. https://doi.org/10.1016/j.ijbiomac.2018.10.133.

Yusop, M. F. M., Ahmad, M. A., Rosli, N. A., Gonawan, F. N., & Abdullah, S. J. (2021). Scavenging malachite green dye from aqueous solution using durian peel based activated carbon. *Malaysian J. Fundam. Appl. Sci*., 17, 95–103. https://doi.org/10.11113/MJFAS.V17N1.2173.

Zoroufchi Benis, K., Motalebi Damuchali, A., McPhedran, K. N., & Soltan, J. (2020). Treatment of aqueous arsenic – A review of biosorbent preparation methods. *J. Environ. Manage*., 273, 111126. https://doi.org/10.1016/j.jenvman.2020.111126.